
STOCHASTIC VARIATIONAL PROPAGATION: LOCAL, SCALABLE AND EFFICIENT ALTERNATIVE TO BACKPROPAGATION

Bojian Yin

Department of Electrical Engineering
Eindhoven University of Technology
The Netherlands
b.yin@tue.nl

Federico Corradi

Department of Electrical Engineering
Eindhoven University of Technology
The Netherlands
f.corradi@tue.nl

ABSTRACT

Backpropagation (BP) is the cornerstone of deep learning, but its reliance on global gradient synchronization limits scalability and imposes significant memory overhead. We propose Stochastic Variational Propagation (SVP), a scalable alternative that reframes training as hierarchical variational inference. SVP treats layer activations as latent variables and optimizes local Evidence Lower Bounds (ELBOs), enabling independent, local updates while preserving global coherence. However, directly applying KL divergence in layer-wise ELBOs risks inter-layer’s representation collapse due to excessive compression. To prevent this, SVP projects activations into low-dimensional spaces via fixed random matrices, ensuring information preservation and representational diversity. Combined with a feature alignment loss for inter-layer consistency, SVP achieves competitive accuracy with BP across diverse architectures (MLPs, CNNs, Transformers) and datasets (MNIST to ImageNet), reduces memory usage by up to 4x, and significantly improves scalability. More broadly, SVP introduces a probabilistic perspective to deep representation learning, opening pathways toward more modular and interpretable neural network design.

1 Introduction

The success of deep learning across a wide range of domains has been substantially driven by backpropagation (BP), a foundational learning algorithm enabling hierarchical representation learning through end-to-end gradient-based optimization [1, 2]. Despite its algorithmic clarity and practical effectiveness, BP requires the exact storage of indeterminate activations and subsequent gradient computation across all layers. This mechanism facilitates global credit assignment [3]; it also introduces a well-known bottleneck called *update-locking* [4, 5], where the weight update of a given layer must wait until both the forward pass through the entire network and the backward pass through deeper layers are complete. Consequently, this global dependency limits asynchronous updating, and imposes substantial memory and computational overhead, ultimately reducing training efficiency and scalability, especially in resource-constrained devices [6, 7, 8].

BP is often seen as biologically implausible and this drives efforts to discover local learning rules for credit assignment in real neural systems [3, 9, 10]. At the same time, neuroscience suggests that feedback connections may approximate global errors via local activity differences [11, 10], hinting at a bioplausible path to deep learning [12, 3]. Yet, these approaches struggle to reconcile local updates with global learning and lack a unifying theoretical framework.

Given this context, a central research question emerges:

“Can we design a theoretical framework capable of decomposing deep neural network training into local (layer-wise) optimizations while retaining the benefits of hierarchical representation learning?”

This question captures a fundamental conflict: while local learning encourages architectural scalability and computational parallelization, effective deep learning relies on non-linear coordination across the entire network. This disconnect

¹Code is available after submission.

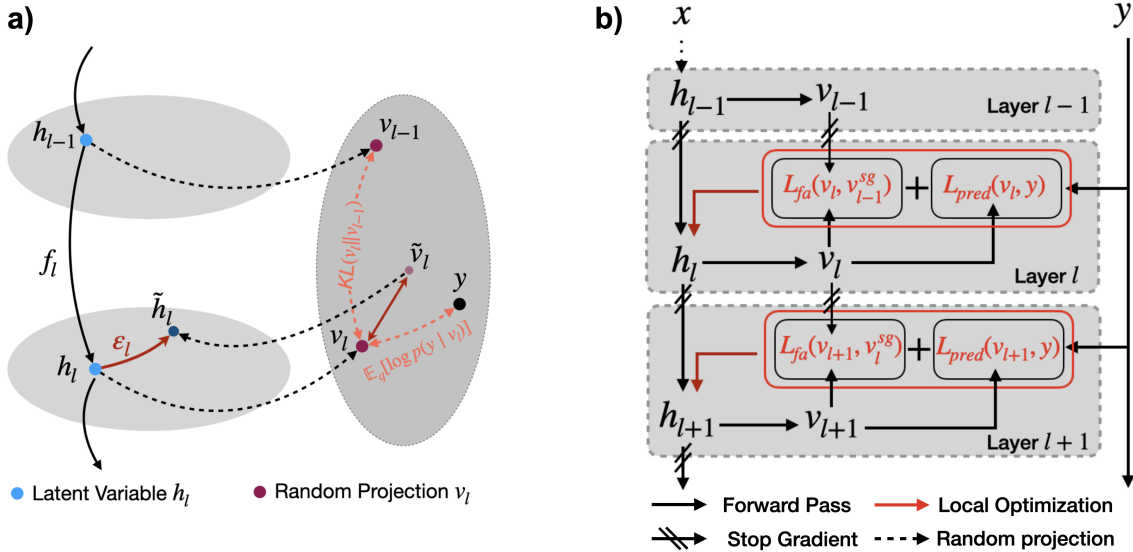


Figure 1: **Overview of Stochastic Variational Propagation (SVP).** (a) SVP treats each hidden activation h_l as a latent variable and projects it to v_l via a random matrix. The local ELBO comprises a log-likelihood term and a KL surrogate that promotes inter-layer consistency. (b) SVP optimizes each layer independently using a prediction loss $\mathcal{L}_{\text{pred}}(v_l, y)$ from the log-likelihood and a feature alignment loss $\mathcal{L}_{\text{fa}}(v_l, v_{l-1}^{\text{sg}})$ approximating the KL term. Arrows denote forward computation (black), local updates (red), and stop-gradient paths (slashed).

often results in misaligned learning signal and suboptimal performance, challenging the network scalability of locally trained models [13].

When information flows through a network, raw inputs are progressively transformed into increasingly disentangled and class-separable representations [14, 15]. This refinement suggests that intermediate layers perform latent inference, selectively preserving task-relevant signals while suppressing redundancy [16]. We formalize this intuition by framing hierarchical representation learning as a probabilistic inference problem, addressing the core tension between global coordination and local updates. Building on variational inference [17], we propose Stochastic Variational Propagation (SVP), a local learning framework that reformulates deep networks as structured latent-variable models. Each layer is modeled as a stochastic latent variable conditioned on its predecessor, turning forward computation into a sequence of local variational inference steps optimized via layer-wise Evidence Lower Bound (ELBO). This enables asynchronous and memory-efficient training without full backpropagation, while preserving global coherence through inter-layer consistency (Fig. 1). Crucially, enforcing a layer-wise ELBO introduces a KL divergence term aligned with the Information Bottleneck (IB) principle [18], encouraging compact representations, but also driving representations toward neural collapse [19, 14]. Instead of weakening the bottleneck, the SVP addresses this collapse by employing fixed random projections guided by the Johnson–Lindenstrauss lemma [20, 15] to approximate variational posteriors within a low-dimensional subspace. These projections serve as implicit regularizers, effectively preventing the collapse by maintaining pairwise distances and preserving representation diversity. Collectively, we show these mechanisms provide a scalable, structured alternative to BP, enabling local learning while preserving global representational structure and inducing qualitatively distinct features compared to BP.

Thus, this work focuses on mathematical analysis, algorithmic development, and experimental evaluations, and the main three contributions are as follows:

- **Theoretical contribution:** we establish a novel layer-wise variational learning framework. We introduce a principled framework for hierarchical objective learning using layer-wise variational inference, supported by a valid variational bound. This approach enables local weight updates and improves the interpretability of the learning process in deep neural networks.
- **Algorithmic contribution:** we proposed SVP and demonstrate its potential as a scalable and efficient alternative to BP. By integrating stochastic random projections, SVP replaces the need for a complete backward pass, thereby facilitating structured local learning.

- **Experimental evaluations:** We demonstrate that SVP scales effectively across architectures and datasets, from MLPs on MNIST to ViTs on ImageNet. Our results show that the SVP algorithm surpasses recently proposed local training methods that address the update locking problem of BP. Moreover, SVP approaches or equals the accuracy performance of BP but with a significant reduction in memory (4× or more).

2 Background

In supervised learning tasks, such as classification applications or regression, neural networks are designed to construct mappings between given input data X and the corresponding target label Y . Traditional feedforward neural networks have a deep structure in which each layer processes the output of the previous layer through a parameterized function. Following the classical formulation [1], such a L -layer neural network can be expressed as a chain of its parameterized sub-functions:

$$f_{1:L}(x) := f(f(\dots f(x, \theta_1) \dots, \theta_{L-1}), \theta_L) \quad (1)$$

where $\theta_i \in \Theta$ represents a set of learnable parameters at layer i . This hierarchical or Markov structure introduces a sequence of hidden representations $\mathcal{H} = [h_1, h_2, \dots, h_L]$ where each representation is defined recursively as $h_i = f(h_{i-1}, \theta_i)$. Given the stacked structure of neural networks, each layer builds on the representation of the previous layer. This structure induces a hierarchical representation where higher layers encode increasingly abstract and task-relevant features. In the following, we review both the deterministic and probabilistic perspective on neural network optimization, together forming the foundation of proposed method.

Backpropagation is the standard approach for network training, aiming to optimize the parameters Θ of the network given a dataset of input-label pairs (x, y) and a task-relevant loss function $\mathcal{L}(h_L, y)$. During training, input data is propagated through the entire network to generate predictions. The loss function then evaluates the network performance by quantifying the distance between these predictions and labels. Next, BP computes the gradient of the loss with respect to each parameter by recursively applying the chain rule in reverse through the network. The update rule for the parameters at layer i , θ_i , are updated iteratively using gradient descent:

$$\theta'_i = \theta_i + \eta \Delta \theta_i; \quad \Delta \theta_i = \frac{\partial \mathcal{L}}{\partial \theta_i} = \frac{\partial \mathcal{L}}{\partial h_i} \cdot \frac{\partial h_i}{\partial \theta_i} = \frac{\partial \mathcal{L}}{\partial h_L} \prod_{j>i} \frac{\partial h_{j+1}}{\partial h_j} \cdot \frac{\partial h_i}{\partial \theta_i} \quad (2)$$

where η is the learning rate. The first term (blue) captures the global contributions of activation h_i to the global loss. It encodes dependencies across all subsequent layers and ensures that updates are coordinated with the global objective. The second term (red) reflects the local sensitivity of h_i with respect to the corresponding parameters θ_i , and can be calculated independently at each layer.

3 Methodology

SVP replaces the global gradient synchronization of BP with a local learning objective, enabling each layer to optimize its parameters independently while preserving inter-layer coherence. By framing network training as a sequence of variational inference steps, it optimizes each layer independently by maximizing a local ELBO on reduced subspace, without waiting for the gradient signal from deeper layers. We now introducing the layerwise ELBO that builds the theoretical foundation of SVP, then describe its optimization via stochastic projection and feature alignment.

3.1 From Forward Propagation to Variational Inference

In principle, BP’s inefficiencies arise from its treatment of activations as fixed, deterministic values that require explicit gradient computations across all layers. In contrast, adopting a probabilistic perspective allows us to view the deep network as hierarchical latent-variable models, in which activations are interpreted as stochastic variables that transform input distributions at different levels of abstraction [21, 22]. Thus, instead of optimizing deterministic activations, learning becomes an inference problem where the goal is to infer their posterior distributions conditioned on observed inputs and outputs. Formally, this corresponds to estimating the *true posterior* over the hidden representations:

$$p(h_1, \dots, h_L | x, y) = \frac{p(y | h_L) p(h_L | h_{L-1}) \dots p(h_1 | x)}{p(y | x)} = \prod_{i=1}^{L+1} p(h_i | h_{i-1}) / p(y|x) \quad (\text{Assumption 1})$$

where $h_0 := x$ and $h_{L+1} := y$. This joint distribution factorizes into a global *evidence* term and a product of local conditional terms. However, computing the evidence term requires marginalization over all hidden representations: $p(y | x) = \int \dots \int \prod_{i=1}^{N+1} p(h_i | h_{i-1}) dh_L \dots dh_1$ which is computationally intractable in high-dimensional deep architecture.

To address this challenge, we apply Variational Inference (VI) [23, 24] to approximate the intractable true posterior $p(y | x)$ with a variational surrogate distribution $q(h)$ by minimizing the Kullback-Leibler (KL) divergence between them in latent space:

$$KL(q(h)||p(h | x)) = \mathbb{E}_q[\log q(h)] - \mathbb{E}_q[\log p(h | x)].$$

This leads to maximizing the Evidence Lower Bound (ELBO):

$$\arg \max_{\theta} \mathcal{E} = \mathbb{E}_q[\log p(y | h)] - KL(q(h)||p(h))$$

where $p(h)$ is the prior distribution over latent variables. At this point, network optimization is reformulated as a structured probabilistic inference problem, which is a fundamental departure from standard BP.

3.2 Layer-wise ELBO

To capture the hierarchical representations of neural network in a probabilistic perspective, we construct a structured variational posterior that mirrors the forward architecture of the model [25]:

$$q(h_1, h_2, \dots, h_L | x, y) = \prod_{i=1}^{L+1} q(h_i | h_{i-1}). \tag{Assumption 2}$$

This formulation retains inter-layer dependencies and avoids the independence assumptions of mean-field VI. It leads to a variational objective:

$$\mathcal{E}_{NN} = \mathbb{E}_q[\log p(y | h_L)] - \sum_{i=1}^N KL(q(h_i | h_{i-1})||p(h_i | h_{i-1})). \tag{Assumption 3}$$

Each term in the sum can be interpreted as a local variational objective, yielding the following layerwise ELBO:

$$\arg \max_{\theta} \mathcal{E}_i = \underbrace{\mathbb{E}_{q(h_i|x,y)} [\log p(y | h_i)]}_{\text{Expected Log-Likelihood}} - \underbrace{KL(q(h_i | h_{i-1})||p(h_i | h_{i-1}))}_{\text{KL Divergence Term}},$$

where the first term encourages the layer to produce class-discriminative representations, and the second term acts as a regularizer that enforces local consistency between adjacent layers by minimizing divergence from the prior. Then, we derive a lower bound for the ELBO of the entire network in the following theorem:

Theorem 1 *The lower bound of global ELBO is given by sum of layer-wise ELBOs: $\frac{1}{L} \sum_{i=1}^L \mathcal{E}_i \leq \mathcal{E}_{NN}$. Proof. (details in the Appendix).* This result ensures that local optimization at each layer contributes meaningfully to the global objective, establishing SVP as a valid alternative to BP.

3.3 Stochastic Variational Propagation

While the ELBO formulation offers a principled training objective, computing the KL divergence terms $KL(q(h_i | h_{i-1})||p(h_i | h_{i-1}))$ is generally intractable in deep networks due to their implicit nature in the network. Moreover, naive KL minimization can overly compress representations and induce Neural Collapse. To address both issues, we introduce a scalable surrogate loss to approximate each layer’s ELBO using randomized compression and cross-layer regularization (as in Figure 1):

$$\arg \min_{\theta} \mathcal{L}_i = \mathcal{L}_{\text{pred}}(R_i h_i, y) + \mathcal{L}_{\text{fa}}(R_i h_i, R_{i-1} h_{i-1}^{sg}),$$

where *sg* means stop gradient, R_i is a fixed random projection matrix to prevent Neural Collapse and enable scalable inference (detailed in 3.3.1), and \mathcal{L}_{fa} is a feature alignment loss for the intractable KL divergence in the ELBO (see 3.3.2). The prediction loss $\mathcal{L}_{\text{pred}}$ encourages task-relevant representations by maximizing the log-likelihood of targets given projected activations, reducing to cross-entropy in supervised tasks. The feature alignment term \mathcal{L}_{fa} regularizes locally by aligning neighboring layer representations, serving as a geometric substitute for backpropagated gradients. Together, these terms offer a practical approximation to hierarchical variational inference while enabling fully decoupled layer-wise training.

3.3.1 Stochastic Random Projection as an controlled Information Bottleneck

Directly minimizing the KL divergence in the layer-wise ELBO naturally induces strong representational compression, risking the emergence of neural collapse. To address this issue, SVP employs fixed random projections, leveraging the Johnson–Lindenstrauss lemma [20] to approximate variational posteriors in a compressed yet expressive subspace. This

approach aligns with the IB principle [18, 26], aiming to preserve task-relevant information while discarding noise, and is supported by evidence that mutual information with labels persists across intermediate layers [16], even under compression. Formally, SVP compresses activations as follows:

$$v_i = R_i h_i, \quad R_i \sim \mathcal{N}(0, \sigma), \quad R_i \in \mathbb{R}^{d' \times d}, \quad d' \ll d. \quad (3)$$

Here, R_i is a fixed random matrix sampled once at initialization. We set d' to the number of classes, forcing alignment with the output space in classification. We formally state the information preservation guarantee of random projections as follows: **Theorem 2.** *Let x denote the network input, assume h_i has bounded second moments. Then, $\forall \varepsilon \in (0, 1)$, if $d' = O(\varepsilon^{-2} \log n)$, the mutual information satisfies, $I(x; v_i) \geq I(x; h_i) - \delta(\varepsilon)$, where $\delta(\varepsilon) \rightarrow 0$ as $\varepsilon \rightarrow 0$. To improve generalization, we apply dropout to the projection weights during training: $v_i = \text{Dropout}(R_i)h_i$. This injects structured noise into the latent space, acting as a Bayesian-inspired regularizer [27]. These stochastic operations implement a Monte Carlo variational approximation, enabling efficient layerwise inference without backpropagation or extra parameters.*

3.3.2 Feature Alignment Loss

An essential component of SVP is ensuring that each layer not only captures task-relevant information, but also maintains coherence with adjacent layers. This inter-layer consistency is critical to preserving the hierarchical structure of deep networks under local optimization, but commonly ignored in most local learning rules [28, 13, 29]. In SVP, this is achieved through a feature alignment loss \mathcal{L}_{fa} , which acts as a tractable surrogate for the intractable KL divergence in the layer-wise ELBO, in format:

$$\mathcal{L}_{\text{fa}} = \|S(v_i) - S(v_{i-1})\|_F^2, \quad (4)$$

where $S(\cdot)$ computes a pairwise cosine similarity matrix over the batch. This loss is invariant to rotation and scaling (under normalization), and encourages the network to preserve geometric consistency across layers.

Theoretical Justification. \mathcal{L}_{fa} approximates the KL divergence between adjacent latent distributions through sample-based alignment. It is related to kernel-based divergence estimates such as Maximum Mean Discrepancy [30] and has been shown to reflect distributional similarity in representation learning [31, 32].

We further establish that normalization is critical for stability of \mathcal{L}_{fa} [33, 34]: **Theorem 3.** *Let h_i be an unnormalized activation with variance σ_i^2 , and $\kappa(h_i)$ the condition number of its covariance matrix. Then, in the high-dimensional limit ($d_i \rightarrow \infty$), there exists $C > 0$ such that: $\mathbb{E}[\mathcal{L}_{\text{fa}}] \geq C \cdot \frac{\kappa(h_i)^2}{\sigma_i^2}$. This implies that poorly conditioned activations will result in explosion of alignment loss. Normalization layers (e.g., BatchNorm [35] or LayerNorm [36]) mitigate this effect by bounding $\kappa(h_i)$, ensuring stable convergence of local ELBO. While we apply cosine-based similarity loss in this work, \mathcal{L}_{fa} can be adapted to contrastive or mutual information-based objectives [16, 37, 38], depending on the architecture and supervision level.*

4 Related Work

The intersection of probabilistic inference and biologically plausible optimization has inspired a range of methods that seek to improve the scalability, interpretability, and local adaptability of deep learning. We organize related work into three areas: variational inference, local learning, and forward-only training.

Variational Inference and Probabilistic Deep Learning. Variational inference (VI) enables tractable approximate Bayesian learning via ELBO maximization [39, 23], foundational to deep generative models like VAEs [21, 40, 41], and their structured extensions [22, 25]. SVP adapts VI for feedforward networks, combining local latent approximations with task-driven learning, and can be seen as a layer-wise variational EM scheme.

Gradient-Based Local Learning Local learning reduces backpropagation overhead by optimizing layers independently, from greedy layer-wise training [8] to local heads [7, 42] and synchronization strategies [43]. Recent blockwise and parallel approaches [13, 28] aim to scale under memory constraints, but often suffer from global feature inconsistency [13]. SVP alleviates this via variational alignment. More biologically inspired alternatives include FA [44], DFA [45], DPK [46], and TP [47], which replace gradients with alternative feedback signals. More recent Hebbian variants [48, 49] show promise for scalable bio-plausible learning, though accuracy and depth remain challenges.

Forward-Only Credit Assignment Forward-only methods eliminate backprop by using dual forward passes, e.g., Forward-Forward (FF)[37], Signal Propagation[38], and PEPITA [50]. Other FF variants [51, 52, 53] reframe credit assignment via L_2 distances. Despite biological inspiration, these methods often face inter-layer misalignment [29], limiting hierarchical feature learning.

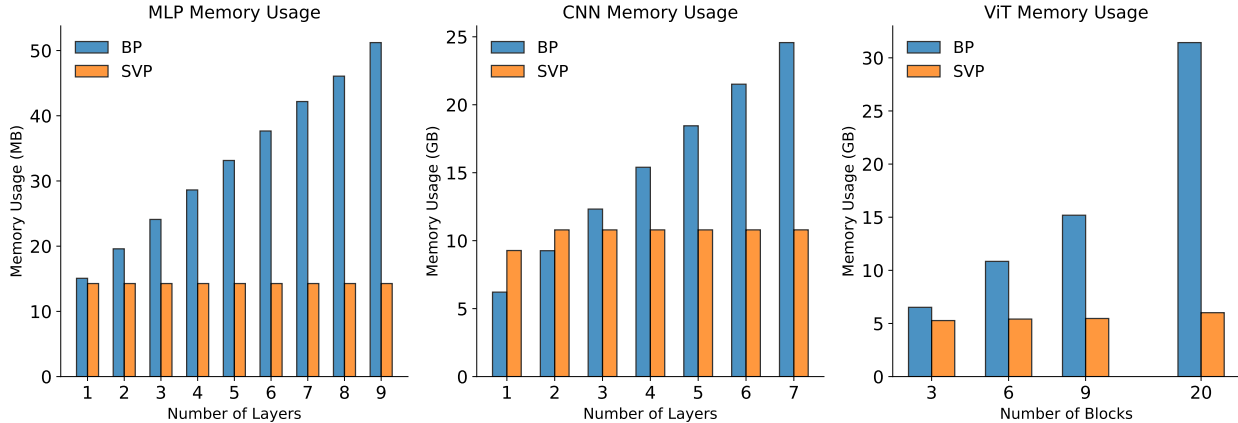


Figure 2: Peak training memory on (a) MLPs (1024 neurons/layer) as a function of depth. BP memory scales linearly, while SVP remains constant; (b) CNNs on the Imagenette without pooling layers. Each convolutional layer uses a kernel size of 3 and 64 output channels; (c) ViTs on Imagenette. For fair comparison, we are using SGD as the optimizer in training.

5 Experiments

We evaluate the effectiveness, interpretability, and scalability of SVP across a range of standard benchmarks. Our experiments include multiple architectures, including MLPs, CNNs, and Vision Transformers (ViTs), and datasets of increasing complexity, from MNIST and CIFAR-10/100 to ImageNette and ImageNet-1K. To assess SVP’s capacity for local learning, we compare it against established local training baselines across multiple network scales. We further extend SVP to block-wise training (SVP+) for ViTs, demonstrating its compatibility with modern large-scale architectures without relying on full backpropagation.

5.1 Experiments on MLPs

We begin by evaluating SVP on fully connected networks trained on benchmarks: MNIST and CIFAR-10/100. These datasets serve as controlled settings to study local learning dynamics in low-dimensional and moderately complex inputs.

Method	Memory	FLOPS	Model	MNIST	CIFAR10	CIFAR100
BP	$\mathcal{O}(NL)$	$\mathcal{O}(N^2L)$	MLP[38]	99.25 ± 0.09	57.80 ± 0.20	30.20 ± 0.10
TP	$\mathcal{O}(NL)$	$\mathcal{O}(N^2L)$	MLP[47]	97.96 ± 0.08	49.64 ± 0.26	-
FA	$\mathcal{O}(NL)$	$\mathcal{O}(NLC)$	MLP[38]	98.36 ± 0.03	53.10 ± 0.30	25.70 ± 0.20
DFA	$\mathcal{O}(NL)$	$\mathcal{O}(NLC)$	MLP[38]	98.26 ± 0.08	57.10 ± 0.20	26.90 ± 0.10
PEPITA	$\mathcal{O}(NL)$	$\mathcal{O}(N^2L)$	MLP[50]	98.01 ± 0.09	52.57 ± 0.36	24.91 ± 0.22
SP	$\mathcal{O}(N)$	$\mathcal{O}(N^2L)$	MLP[38]	98.29 ± 0.03	57.38 ± 0.16	29.70 ± 0.19
SVP	$\mathcal{O}(N)$	$\mathcal{O}(NLC)$	MLP	99.32 ± 0.05	61.43 ± 0.31	32.95 ± 0.26

Table 1: Performance and complexity of SVP vs. local learning methods on MNIST, CIFAR-10, and CIFAR-100 with MLPs. Memory and FLOPS scale with N (neurons/layer), L (layers), and C (classes). Results are mean ± std over 3 runs.

Accuracy and Efficiency. To establish a comprehensive comparison, we evaluate SVP alongside a range of biologically motivated and local learning algorithms that do not rely on full BP. All models are trained with identical architectures and training schedules to ensure a fair comparison. As shown in Table 1, SVP consistently outperforms all local learning baselines, despite operating under reduced memory and computational budgets. In particular, SVP even surpasses BP on these datasets while requiring fewer operations and avoiding global gradient synchronization. Moreover, Figure 2(a) confirms SVP’s memory efficiency during training. The training memory usage of SVP remains effectively constant as the depth of the network increases, in contrast to its theoretical complexity reported in Table 1.

Representation Visualization. We analyze the internal representations of the network trained by SVP in Figure 3 and A6. In general, input features are initially entangled, deeper layers show improved class separation. It is obvious that v_i forms sharper, more distinct clusters than h_i , indicating that random projections not only preserve but often enhance class-discriminative structure.

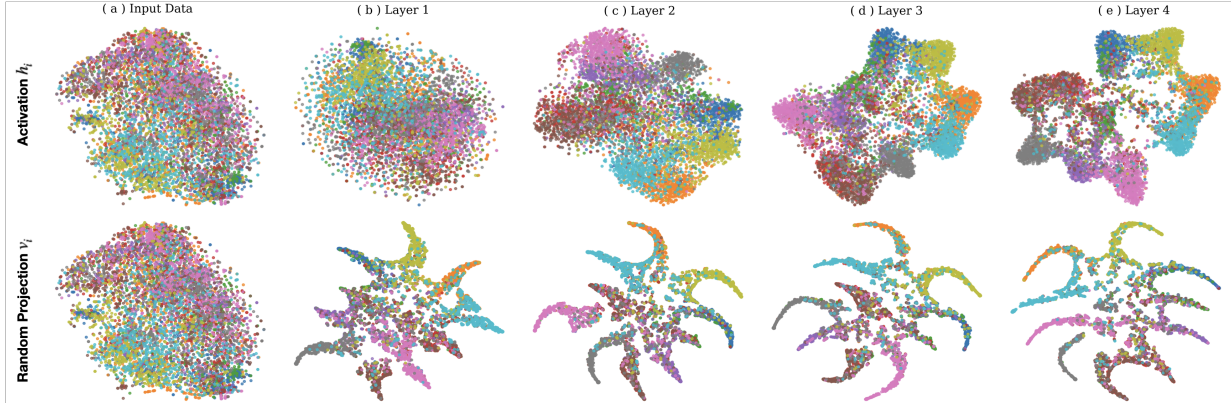


Figure 3: t-SNE visualization of activations and random projections on CIFAR-10, colored by class.

Ablation study. We further investigate the effect of projection dimension and network width on SVP performance (Figure 4b,c). Increasing the projection dimension d improves test accuracy, with diminishing returns beyond $d = 700$, suggesting a trade-off between representational precision and efficiency. Likewise, wider networks result in faster convergence and higher accuracy on CIFAR-100, with improvements saturating above 800 neurons. These trends are consistent with our theoretical insights (Theorem 4 ??), which indicate that high-dimensional layers reduce alignment loss and preserve inter-layer information. Together, these findings highlight the role of capacity and compression in enabling stable local learning with SVP.

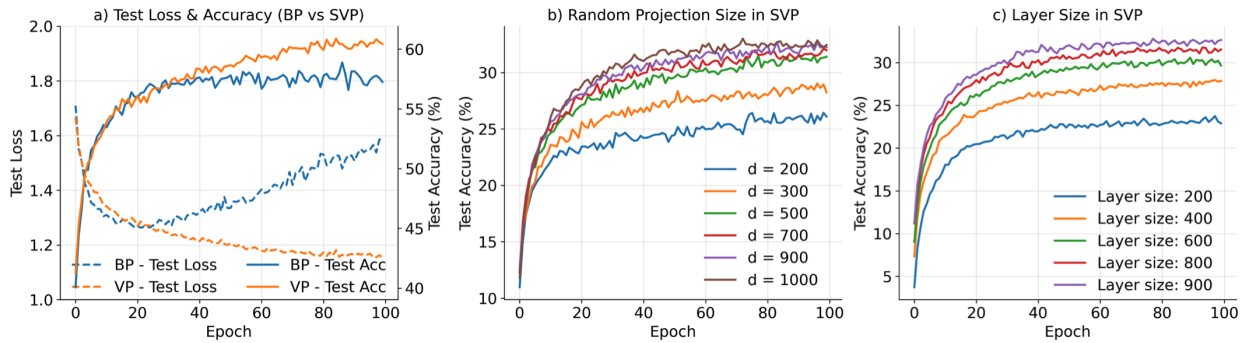


Figure 4: (a) Training curves of a 3-layer MLP on CIFAR-10: SVP achieves lower test loss, higher accuracy, and more stable convergence than BP. Ablation study: (b) random projection dimension in a 3×1000 MLP trained on CIFAR-100; activations are downsampled via adaptive pooling before projection. (c) network width in SVP on CIFAR-100, showing that wider layers significantly enhance performance and stability.

5.2 Scaling SVP to CNNs

We next explore how SVP can scale effectively to convolutional architectures despite discarding explicit spatial structure when utilizing fully connected random projection. To this end, we evaluate SVP on a VGG-11 architecture and compare it against representative local learning methods, forward-only training algorithms, and conventional global BP.

Accuracy. Table 2 reports the test accuracies in F-MNIST, CIFAR-10/100 and Tiny-Imagenet. SVP-CNN performs competitively BP, achieving within 1–2% of BP on small-scale datasets like F-MNIST, CIFAR-10/100, and even slightly surpassing it on F-MNIST. In particular, SVP outperforms all local and forward-only baselines on all given tasks, including DFA [45], DKP [46], SoftHebb [48], and TFF [52]. In the more challenging Tiny-ImageNet benchmark, SVP

Model	F-MNIST	CIFAR10	CIFAR100	Imagenette	Tiny-Imagenet
BP-CNN	93.52 ± 0.22	91.58 ± 0.53	68.7 ± 0.38	90.5 ± 0.45	60.80
Local Learning					
FA [45]	91.12 ± 0.39	60.45 ± 1.13	19.49 ± 0.97	-	-
DFA [45]	91.54 ± 0.14	62.70 ± 0.36	48.03 ± 0.61	-	17.47 ± 0.34
DKP [46]	91.66 ± 0.27	64.69 ± 0.72	52.62 ± 0.48	-	25.36 ± 0.82
Softhebb [48]	-	80.3	56	81.0	-
SGR [13]	-	72.40 ± 0.75	49.41 ± 0.44	-	-
LLS[28]	90.54 ± 0.23	88.64 ± 0.12	58.84 ± 0.33	-	35.99 ± 0.38
Forward-Only					
FF-CNN [37]	-	59	-	-	-
Symba [53]	-	59.09	28.28	-	-
TFF [52]	91.44 ± 0.49	83.51 ± 0.78	35.26 ± 0.23	-	-
PEPITA [50]	-	56.33 ± 1.35	27.56 ± 0.60	-	-
DF-R [51]	92.5	84.75	48.16	81.2	-
SVP-CNN	93.67 ± 0.17	91.36 ± 0.32	67.12 ± 0.18	88.09 ± 0.73	42.48 ± 0.65

Table 2: Comparison of test accuracies across various datasets, values are mean ± std over 3 runs.

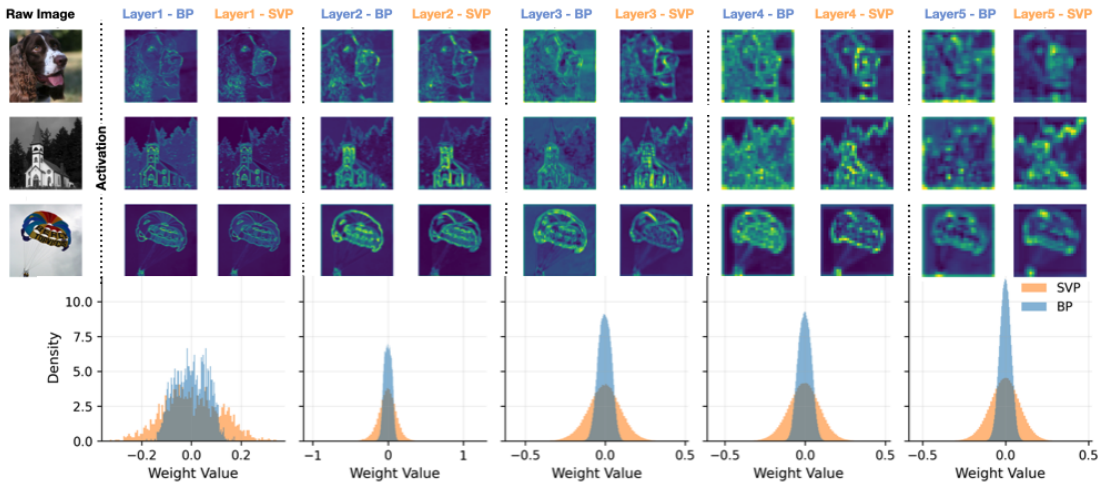


Figure 5: Activation maps and weight distributions from a VGG-11 network trained with BP and SVP on Imagenette. Top: SVP produces structured and class-distinct activations comparable to BP. Bottom: SVP-trained weights (orange) exhibit broader distributions than BP (blue), indicating more distributed use of parameters.

achieves a top-1 accuracy of 42.48%. Although this performance still exceeds that of many local learning baselines, it indicates current limitations in scaling SVP to large numbers of classes. This gap may arise from the bottleneck introduced by random projection and premature exposure of early layers to label supervision, both of which are increasingly critical as the number of target classes grows and task complexity rises.

Training memory efficiency. Figure 2(b) illustrates the training memory usage of SVP and BP on CNNs. While SVP exhibits a clear memory advantage in MLPs, its benefit is more moderate in CNNs. This is because convolution operations are inherently sparse and memory-efficient, while the dense random projections used in SVP introduce additional overhead. However, SVP still maintains a significant advantage in deeper architectures.

Feature visualization. Figure 5 indicates that SVP effectively learns high-quality spatial and discriminative representations, despite discarding explicit spatial priors. Compared with BP, the broader weight distributions from SVP suggest robust and distributed encoding. These results support SVP as a scalable and efficient alternative to backpropagation.

5.3 Scaling to Vision Transformer

While SVP converges when optimizing CNNs, the sparsity and weight sharing in convolutional layers can mask its computational and memory advantages. To more efficiently assess the scalability of SVP, we extend it to the Vision

Transformer (ViT) [54], whose dense MLP-like blocks make it ideal for stress testing large memory requirements during training.

To scale to the Vision Transformers models, we propose SVPⁱ⁺, a blockwise variant of SVP tailored for large MLP-based architectures. A transformer is split into i units where each unit is optimized independently via local objective. This design aligns with the residual structure of ViT while preserving the localized memory and learning advantage of SVP. SVP+ leverages the class token or mean over all tokens as a stable and semantically rich representation for local supervision, enabling efficient classification without end-to-end backpropagation. Table 3 demonstrates accuracy and peak memory usage of SVP+. SVP+ maintains substantial memory savings in ViTs, while preserving accuracy, with memory usage remaining nearly constant with increasing block depth (Figure 2(c)). This trend is similar to the MLP findings and demonstrates SVP scalability across architectures. Compared to BP, SVP+ reduces training memory by 64%–75% without sacrificing stability or model capacity.

Task	Method	Test Acc	Memory(GB)
CIFAR-10	BP	93.62	3.05
	SVP ⁷⁺	92.17	1.18 (↓ 64.1%)
CIFAR-100	BP	75.24	3.05
	SVP ⁷⁺	74.27	1.18 (↓ 64.1%)
Imagenette	BP	92.82	22.12
	SVP ⁷⁺	92.25	5.43 (↓ 75.45%)
Imagenet	BP [55]	79.4	20.70
	BL ³⁺ [13]	78.65	11.73(↓ 43.33%)
	SVP ³⁺	72.43*	6.54 (↓ 68.41%)
	SVP ¹²⁺	59.62*	4.30 (↓ 79.22%)

Table 3: Experimental results. ‘Memory’ refers to GPU training memory usage with batch sizes of 128 and 256 on ImageNet.

6 Discussion and Conclusions

In conclusion, we introduce SVP, a scalable and memory-efficient alternative to BP that reformulates training as local variational inference. By combining local ELBO optimization with random projection, SVP enables parallel, asynchronous updates while preserving global coherence without introducing extra trainable parameters. Compared to backpropagation, SVP achieves competitive accuracy with up to 4× memory efficiency, and consistently outperforms prior local learning methods. It generalizes effectively across MLPs, CNNs, and ViTs, scaling from small to moderately large vision tasks. Beyond training efficiency, SVP also provides a structured probabilistic view of deep representations, offering a foundation for interpretable learning dynamics and architecture design grounded in information flow. It’s worth mentioning that the SVP also draws conceptual parallels with Equilibrium Propagation [9] and energy-based models. Both frameworks enable local updates that align with global objectives, but they operate through distinct mechanisms: variational inference for SVP and dynamical relaxation for EP. Bridging these perspectives under a unified probabilistic or dynamical systems framework is an interesting direction for future research.

The above results reveal interesting weaknesses of SVP that suggest several directions for future work. First, the Markov assumption between layers, while simplifying inference, may limit expressivity in architectures with long-range dependencies such as residual connections. Second, the absence of second-order gradient information may reduce SVP’s effectiveness in navigating ill-conditioned loss surfaces. Third, SVP’s reliance on local supervision may limit convergence in large-scale classification tasks where informative gradients may only emerge in later layers. Finally, aggressive dimension reduction via random projection may lead to information loss in narrow architectures. Addressing these challenges through more expressive dependency modeling, adaptive projection schemes, and architecture-aware supervision could extend the applicability of SVP to broader research.

Acknowledgments

The authors gratefully acknowledge the helpful discussions with Sander Bohte and Henk Corporaal. This work has been funded by the Dutch Organization for Scientific Research (NWO) with Grant KICH1.ST04.22.021

References

[1] David E Rumelhart, Geoffrey E Hinton, and Ronald J Williams. Learning representations by back-propagating errors. *nature*, 323(6088):533–536, 1986.

[2] Yann LeCun, Yoshua Bengio, and Geoffrey Hinton. Deep learning. *nature*, 521(7553):436–444, 2015.

- [3] Timothy P Lillicrap, Adam Santoro, Luke Marris, Colin J Akerman, and Geoffrey Hinton. Backpropagation and the brain. *Nature Reviews Neuroscience*, 21(6):335–346, 2020.
- [4] Max Jaderberg, Wojciech Marian Czarnecki, Simon Osindero, Oriol Vinyals, Alex Graves, David Silver, and Koray Kavukcuoglu. Decoupled neural interfaces using synthetic gradients. In *International conference on machine learning*, pages 1627–1635. PMLR, 2017.
- [5] Andreas Griewank and Andrea Walther. *Evaluating derivatives: principles and techniques of algorithmic differentiation*. SIAM, 2008.
- [6] Xiangzhong Luo, Di Liu, Hao Kong, Shuo Huai, Hui Chen, Guochu Xiong, and Weichen Liu. Efficient deep learning infrastructures for embedded computing systems: A comprehensive survey and future envision. *ACM Transactions on Embedded Computing Systems*, 24(1):1–100, 2024.
- [7] Eugene Belilovsky, Michael Eickenberg, and Edouard Oyallon. Greedy layerwise learning can scale to imagenet. In *International conference on machine learning*, pages 583–593. PMLR, 2019.
- [8] Yoshua Bengio, Pascal Lamblin, Dan Popovici, and Hugo Larochelle. Greedy layer-wise training of deep networks. *Advances in neural information processing systems*, 19, 2006.
- [9] Benjamin Scellier and Yoshua Bengio. Equilibrium propagation: Bridging the gap between energy-based models and backpropagation. *Frontiers in computational neuroscience*, 11:24, 2017.
- [10] Jordan Guerguiev, Timothy P Lillicrap, and Blake A Richards. Towards deep learning with segregated dendrites. *elife*, 6:e22901, 2017.
- [11] James CR Whittington and Rafal Bogacz. Theories of error back-propagation in the brain. *Trends in cognitive sciences*, 23(3):235–250, 2019.
- [12] João Sacramento, Rui Ponte Costa, Yoshua Bengio, and Walter Senn. Dendritic cortical microcircuits approximate the backpropagation algorithm. *Advances in neural information processing systems*, 31, 2018.
- [13] Yibo Yang, Xiaojie Li, Motasem Alfarra, Hasan Hammoud, Adel Bibi, Philip Torr, and Bernard Ghanem. Towards interpretable deep local learning with successive gradient reconciliation. In *Proceedings of the 41st International Conference on Machine Learning*, pages 56196–56215, 2024.
- [14] Hangfeng He and Weijie J Su. A law of data separation in deep learning. *Proceedings of the National Academy of Sciences*, 120(36):e2221704120, 2023.
- [15] Xiang Wang, Rebecca Roelofs, Shuyang Song, Yair Carmon, and John C Duchi. Representation projection invariance mitigates representation collapse. *arXiv preprint arXiv:2205.11603*, 2022.
- [16] Ravid Shwartz-Ziv and Naftali Tishby. Opening the black box of deep neural networks via information. *arXiv preprint arXiv:1703.00810*, 2017.
- [17] Martin J Wainwright, Michael I Jordan, et al. Graphical models, exponential families, and variational inference. *Foundations and Trends® in Machine Learning*, 1(1–2):1–305, 2008.
- [18] Naftali Tishby, Fernando C Pereira, and William Bialek. The information bottleneck method. *arXiv preprint physics/0004057*, 2000.
- [19] Vardan Papayan, XY Han, and David L Donoho. Prevalence of neural collapse during the terminal phase of deep learning training. *Proceedings of the National Academy of Sciences*, 117(40):24652–24663, 2020.
- [20] William B Johnson, Joram Lindenstrauss, et al. Extensions of lipschitz mappings into a hilbert space. *Contemporary mathematics*, 26(189-206):1, 1984.
- [21] Diederik P. Kingma and Max Welling. Auto-encoding variational bayes. In *International Conference on Learning Representations (ICLR)*, 2014.
- [22] Casper Kaae Sønderby, Tapani Raiko, Lars Maaløe, Søren Kaae Sønderby, and Ole Winther. Ladder variational autoencoders. *Advances in neural information processing systems*, 29, 2016.
- [23] David M Blei, Alp Kucukelbir, and Jon D McAuliffe. Variational inference: A review for statisticians. *Journal of the American statistical Association*, 112(518):859–877, 2017.
- [24] Rajesh Ranganath, Sean Gerrish, and David Blei. Black box variational inference. In *Artificial intelligence and statistics*, pages 814–822. PMLR, 2014.
- [25] Arash Vahdat and Jan Kautz. Nvae: A deep hierarchical variational autoencoder. *Advances in neural information processing systems*, 33:19667–19679, 2020.
- [26] Naftali Tishby and Noga Zaslavsky. Deep learning and the information bottleneck principle. In *2015 IEEE information theory workshop (itw)*, pages 1–5. Ieee, 2015.

- [27] Yarin Gal and Zoubin Ghahramani. Dropout as a bayesian approximation: Representing model uncertainty in deep learning. In *international conference on machine learning*, pages 1050–1059. PMLR, 2016.
- [28] Marco Paul E Apolinario, Arani Roy, and Kaushik Roy. Lls: local learning rule for deep neural networks inspired by neural activity synchronization. *arXiv preprint arXiv:2405.15868*, 2024.
- [29] Guy Lorberbom, Itai Gat, Yossi Adi, Alexander Schwing, and Tamir Hazan. Layer collaboration in the forward-forward algorithm. In *Proceedings of the AAAI Conference on Artificial Intelligence*, volume 38, pages 14141–14148, 2024.
- [30] Arthur Gretton, Karsten M Borgwardt, Malte J Rasch, Bernhard Schölkopf, and Alexander Smola. A kernel two-sample test. *The Journal of Machine Learning Research*, 13(1):723–773, 2012.
- [31] Simon Kornblith, Mohammad Norouzi, Honglak Lee, and Geoffrey Hinton. Similarity of neural network representations revisited. In *International conference on machine learning*, pages 3519–3529. PMLR, 2019.
- [32] Aude Genevay, Gabriel Peyré, and Marco Cuturi. Learning generative models with sinkhorn divergences. In *International Conference on Artificial Intelligence and Statistics*, pages 1608–1617. PMLR, 2018.
- [33] Xiang Li, Shuo Chen, Xiaolin Hu, and Jian Yang. Understanding the disharmony between dropout and batch normalization by variance shift. In *Proceedings of the IEEE/CVF conference on computer vision and pattern recognition*, pages 2682–2690, 2019.
- [34] Shibani Santurkar, Dimitris Tsipras, Andrew Ilyas, and Aleksander Madry. How does batch normalization help optimization? *Advances in neural information processing systems*, 31, 2018.
- [35] Sergey Ioffe and Christian Szegedy. Batch normalization: Accelerating deep network training by reducing internal covariate shift. In *International conference on machine learning*, pages 448–456. pmlr, 2015.
- [36] Jimmy Lei Ba, Jamie Ryan Kiros, and Geoffrey E Hinton. Layer normalization. *arXiv preprint arXiv:1607.06450*, 2016.
- [37] Geoffrey Hinton. The forward-forward algorithm: Some preliminary investigations. *arXiv preprint arXiv:2212.13345*, 2022.
- [38] Adam Kohan, Edward A Rietman, and Hava T Siegelmann. Signal propagation: The framework for learning and inference in a forward pass. *IEEE Transactions on Neural Networks and Learning Systems*, 2023.
- [39] Michael I Jordan, Zoubin Ghahramani, Tommi S Jaakkola, and Lawrence K Saul. An introduction to variational methods for graphical models. *Machine learning*, 37:183–233, 1999.
- [40] Kihyuk Sohn, Honglak Lee, and Xinchen Yan. Learning structured output representation using deep conditional generative models. *Advances in neural information processing systems*, 28, 2015.
- [41] Irina Higgins, Loic Matthey, Arka Pal, Christopher Burgess, Xavier Glorot, Matthew Botvinick, Shakir Mohamed, and Alexander Lerchner. beta-vae: Learning basic visual concepts with a constrained variational framework. In *International conference on learning representations*, 2017.
- [42] Arild Nøkland and Lars Hiller Eidnes. Training neural networks with local error signals. In *International conference on machine learning*, pages 4839–4850. PMLR, 2019.
- [43] Maxence M Ernout, Fabrice Normandin, Abhinav Moudgil, Sean Spinney, Eugene Belilovsky, Irina Rish, Blake Richards, and Yoshua Bengio. Towards scaling difference target propagation by learning backprop targets. In *International Conference on Machine Learning*, pages 5968–5987. PMLR, 2022.
- [44] Timothy P Lillicrap, Daniel Cownden, Douglas B Tweed, and Colin J Akerman. Random synaptic feedback weights support error backpropagation for deep learning. *Nature communications*, 7(1):13276, 2016.
- [45] Arild Nøkland. Direct feedback alignment provides learning in deep neural networks. *Advances in neural information processing systems*, 29, 2016.
- [46] Matthew Bailey Webster, Jonghyun Choi, and Changwook Ahn. Learning the connections in direct feedback alignment. *openreview*, 2021.
- [47] Dong-Hyun Lee, Saizheng Zhang, Asja Fischer, and Yoshua Bengio. Difference target propagation. In *Proceedings of the 2015th European Conference on Machine Learning and Knowledge Discovery in Databases-Volume Part I*, pages 498–515, 2015.
- [48] Adrien et al. Journé. Hebbian deep learning without feedback. In *ICLR2023*, 2023.
- [49] Manu Srinath Halvagal and Friedemann Zenke. The combination of hebbian and predictive plasticity learns invariant object representations in deep sensory networks. *Nature Neuroscience*, 26(11):1906–1915, 2023.

- [50] Giorgia DellaFerrera and Gabriel Kreiman. Error-driven input modulation: solving the credit assignment problem without a backward pass. In *International Conference on Machine Learning*, pages 4937–4955. PMLR, 2022.
- [51] Yujie Wu, Siyuan Xu, Jibin Wu, Lei Deng, Mingkun Xu, Qinghao Wen, and Guoqi Li. Distance-forward learning: Enhancing the forward-forward algorithm towards high-performance on-chip learning. *arXiv preprint arXiv:2408.14925*, 2024.
- [52] Thomas Dooms, Ing Jyh Tsang, and Jose Oramas. The trifecta: Three simple techniques for training deeper forward-forward networks. *arXiv preprint arXiv:2311.18130*, 2023.
- [53] Heung-Chang Lee and Jeonggeun Song. Symba: Symmetric backpropagation-free contrastive learning with forward-forward algorithm for optimizing convergence. *arXiv:2303.08418*, 2023.
- [54] Alexey Dosovitskiy, Lucas Beyer, Alexander Kolesnikov, Dirk Weissenborn, Xiaohua Zhai, Thomas Unterthiner, Mostafa Dehghani, Matthias Minderer, Georg Heigold, Sylvain Gelly, et al. An image is worth 16x16 words: Transformers for image recognition at scale. *arXiv preprint arXiv:2010.11929*, 2020.
- [55] Li Yuan, Yunpeng Chen, Tao Wang, Weihao Yu, Yujun Shi, Zi-Hang Jiang, Francis EH Tay, Jiashi Feng, and Shuicheng Yan. Tokens-to-token vit: Training vision transformers from scratch on imagenet. In *Proceedings of the IEEE/CVF international conference on computer vision*, pages 558–567, 2021.

A Appendix

Appendix Contents

- A.1 Algorithm
- A.2 Additional Experimental Results
- A.3 Proofs of Theorems
- A.4 Model Architecture and Experiment Details
- A.5 Ethic Statement

A.1 Algorithm

Algorithm 1 Stochastic Variational Propagation

Require: Training batch data (x, y) , learning rate η , random projection matrix $R_l \sim \mathcal{N}$

Ensure: Updated network weights θ

```

1: for each layer  $l$  from 1 to  $L - 1$  do
2:   Detach From above layer:  $h_{l-1} = h_{l-1}.detach()$ 
3:   Update activation:  $h_l \leftarrow f(h_{l-1}, \theta_l)$ 
4:   Approximate  $\partial h_l$ :
5:     Random Projection:  $v_l = dp(R_l)h_l$  or  $v_l = dp(R_l)[h_l, y]$ 
6:     Loss:  $\mathcal{L}_l \leftarrow L_{Pred}(v_l, y) + L_{fa}(v_l, v_{l-1})$ 
7:     Activation drift:  $\varepsilon_l \leftarrow \frac{\partial \mathcal{L}_l}{\partial h_l}$ 
8:     Weight Update:  $\theta_l \leftarrow \theta_l - \eta \cdot \frac{\partial h_l}{\partial \theta_l} \varepsilon_l$ 
9:     Clear unnecessary tensors
10: end for
11:  $h_{L-1} = h_{L-1}.detach()$ 
12:  $h_L \leftarrow f(h_{L-1}, \theta_L)$ 
13: Loss:  $\mathcal{L}_L \leftarrow L_{Pred}(h_L, y) + L_{fa}(h_L, v_{L-1})$ 
14:  $\theta_L \leftarrow \theta_L - \eta \cdot \frac{\partial \mathcal{L}_L}{\partial \theta_L}$ 

```

Activation drift is The first term (blue) captures the global contributions of activation h_i to the global loss in Eq:2.

A.2 Additional Experimental Results

A.2.1 MNIST feature visualization

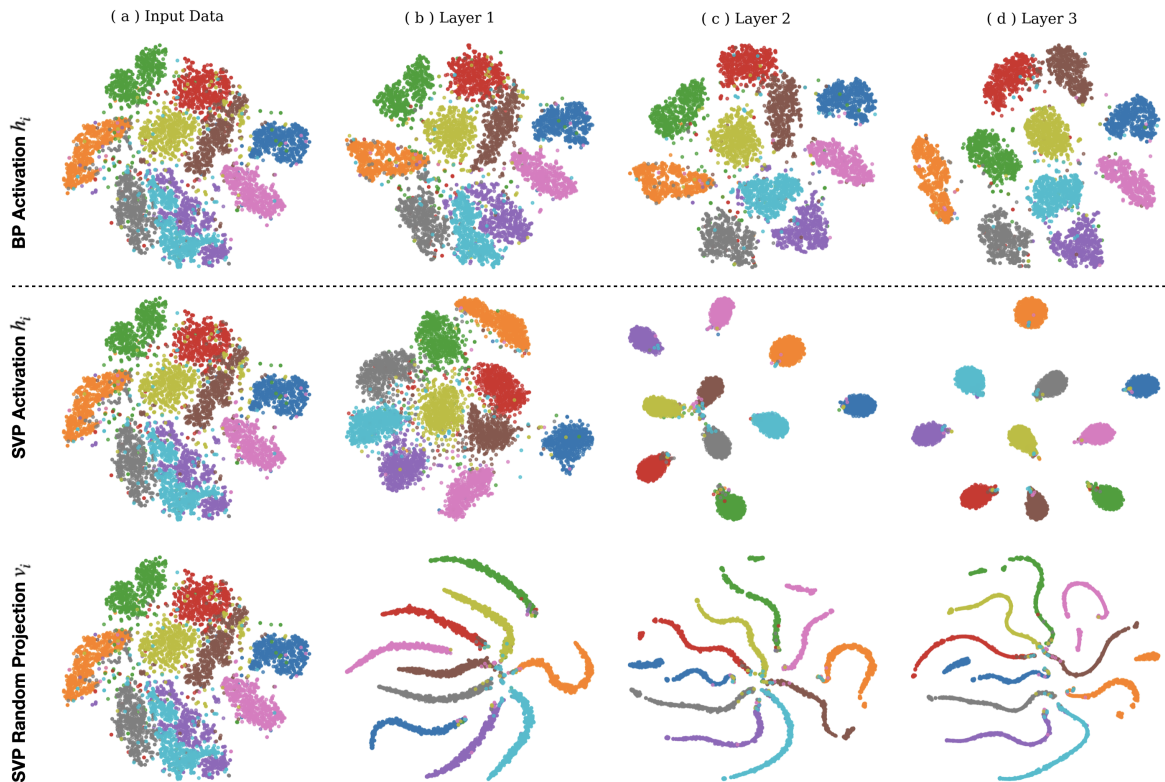


Figure A6: t-SNE visualization of MNIST representations. Each color indicates a digit class. **Top:** Layer-wise activations h_i from a network trained with BP. **Middle:** Activations from a network trained with SVP. **Bottom:** Corresponding random projections $v_i = R_i h_i$ from SVP. SVP leads to more compact and class-separable features, with random projections preserving and enhancing this structure.